Medical Engineering & Physics 33 (2011) 924–933

Contents lists available at ScienceDirect

Medical Engineering & Physics

journal homepage: www.elsevier.com/locate/medengphy

Fast 3D reconstruction of the spine from biplanar radiographs using a deformable articulated model

Daniel C. Moura [a,b,*], Jonathan Boisvert [c,d], Jorge G. Barbosa [a,b], Hubert Labelle [e], João Manuel R.S. Tavares [f,g]

[a] Universidade do Porto, Faculdade Engenharia, Departamento de Engenharia Informática, Porto, Portugal
[b] Laboratório de Inteligência Artificial e de Ciência de Computadores, Porto, Portugal
[c] National Research Council Canada, Ottawa, Canada
[d] École Polytechnique de Montréal, Montréal, Québec, Canada
[e] Sainte-Justine Hospital Research Center, Montréal, Québec, Canada
[f] Universidade do Porto, Faculdade Engenharia, Departamento de Engenharia Mecânica, Porto, Portugal
[g] Instituto de Engenharia Mecânica e Gestão Industrial, Porto, Portugal

ARTICLE INFO

Article history:
Received 26 July 2010
Received in revised form 28 February 2011
Accepted 2 March 2011

Keywords:
3D reconstruction
X-ray imaging
Statistical shape models
Optimisation
Spine
Scoliosis

ABSTRACT

This paper proposes a novel method for fast 3D reconstructions of the scoliotic spine from two planar radiographs. The method uses a statistical model of the shape of the spine for computing the 3D reconstruction that best matches the user input (about 7 control points per radiograph). In addition, the spine was modelled as an articulated structure to take advantage of the dependencies between adjacent vertebrae in terms of location, orientation and shape.

The accuracy of the method was assessed for a total of 30 patients with mild to severe scoliosis (Cobb angle [22°, 70°]) by comparison with a previous validated method. Reconstruction time was 90 s for mild patients, and 110 s for severe. Results show an accuracy of ~0.5 mm locating vertebrae, while orientation accuracy was up to 1.5° for all except axial rotation (3.3° on moderate and 4.4° on severe cases). Clinical indices presented no significant differences to the reference method (Wilcoxon test, $p \leq 0.05$) on patients with moderate scoliosis. Significant differences were found for two of the five indices ($p = 0.03$) on the severe cases, while errors remain within the inter-observer variability of the reference method.

Comparison with state-of-the-art methods shows that the method proposed here generally achieves superior accuracy while requiring less reconstruction time, making it especially appealing for clinical routine use.

1. Introduction

Three-dimensional (3D) assessment of spine deformities is required for properly evaluating scoliosis [1]. However, conventional 3D imaging techniques (i.e. CT – computer tomography and MRI – magnetic resonance imaging) are not suitable for this purposes because they require patients to be lying supine, which alters the global shape of the spine [2]. Additionally, they are expensive and, in the case of CT, a full scan of the spine results in a considerable dose of radiation for the patient [3].

To obtain 3D reconstructions of the spine in standing position, several authors have proposed computational methods that use two (or more) planar radiographs, previously calibrated with a multi-planar radiography calibration system (e.g. [4–8]). Reconstructions from multi-planar radiography allow clinicians to have access to 3D measurements (e.g. plane of maximum deformity [1]) and have been successfully employed for evaluating the effect of different therapeutic approaches (e.g. Boston braces [9] and surgery [10]), predicting the progression of scoliosis [11] and designing more effective braces [12].

Most of the reconstruction methods are based on the identification of several anatomical landmarks on posterior–anterior (PA) and lateral (LAT) radiographs. Currently, computational reconstructions of the spine are achieved by manually identifying a set of 6 stereo-corresponding points per vertebra on the PA and LAT [13–15]. These six points are the centre of superior and inferior endplates, and the superior and inferior extremities of the pedicles. The 3D coordinates of these points are found by triangulation and allow to determine the location and orientation of each vertebra. The location of each vertebra, typically defined as the centre

* Corresponding author at: Faculdade de Engenharia da Universidade do Porto, Departamento de Engenharia Informática, Rua Dr. Roberto Frias, s/n, 4200-465 Porto, Portugal. Tel.: +351 225081888; fax: +351 225574103.
E-mail address: daniel.moura@fe.up.pt (D.C. Moura).

1350-4533/$ – see front matter © 2011 IPEM. Published by Elsevier Ltd. All rights reserved.
doi:10.1016/j.medengphy.2011.03.007

of the endplates [1] or the centre of the four pedicles' landmarks [16], is used to define the vertebral body line, which enables to calculate regional, spinal and global indices of spine deformity, as defined in [1]. The orientation of each vertebra is determined following the standardized frame of reference defined in [1]. The 3D coordinates of the six points are also utilised for recovering vertebrae shape by deforming dense generic vertebral models using dual kriging [17]. For improving the accuracy of the shape of the reconstructed vertebrae and, thus, improving the assessment of local deformities, other studies [18–21] proposed increasing the set of manually identified points by including landmarks that are visible in only one of the radiographs. Both methods require expert users for accurately pinpointing an extended set of landmarks. However, even for experts, it is difficult to find the exact location of the landmarks and to ensure stereo-correspondence, thus, jeopardising reproducibility. Moreover, these procedures are error-prone and very time-consuming.

Several methods have been proposed for addressing the aforementioned problems, in particular, for decreasing user-interaction while increasing reproducibility. In [22] the user interaction time for reconstructing a 3D model was decreased to less than 20 min by requiring a set of 4 landmarks per vertebra in each radiograph (non stereo-correspondent) and using statistical inference for determining vertebrae shape and axial rotation, followed by manual adjustments for refining the reconstruction. However, the amount of user interaction is still very high for clinical routine use, and remains very user-dependent. On the other hand, attempts for automating reconstructions based on 2D/3D registration of deformable vertebrae models [23,24] show that the success of the procedure is largely dependent on the initial solution. Additionally, automated methods only show reconstructions for the lower part of the spine, where radiographs are clearer and with less overlapping structures, but computation of most of the clinical indices require all thoracic and lumbar vertebrae [15].

Very recently, new methods have arisen that try to decrease user interaction by requesting the identification of the spine midline on two radiographs by the means of cubic splines. In [25], the operator adjusts the scale and location of the first and last vertebrae (C7 and L5), which are used for interpolating location and scale of the remaining vertebrae along the 3D spline. Then, an operator manually adjusts each vertebra. Average interaction time was 5 min. In [26], the splines, as well as additional user input (i.e. location, size and orientation of predefined endplates, and position and shape of the apical, T1 and L5 vertebrae), are used as predictors for inferring the shape of the spine using multi-linear regression. A trained operator requires about 2.5 min for performing a fast reconstruction, although it is possible to refine reconstructions, increasing interaction time to 10 min. Both these methods still require considerable user-interaction, making their reconstructions user-dependent and potentially less reproducible. In [27], operators only need to identify the spine midline. However, a 2D approach is used where training and prediction of the spine shape is done independently for each radiograph. This approach is therefore limited since the predicted landmarks on the two radiographs are not related and, additionally, their location depends on the positioning of both patient and X-ray source during the examination.

Kadoury et al. also proposed a statistical approach to obtain a model of the spine from two cubic splines [28]. Local linear embedding (LLE) [29] was used for mapping 3D splines to a lower-dimensional space, which was then used to infer the spine reconstruction using support vector regression (SVR). A total of 732 spine reconstructions were employed for computing both the LLE and the 306 SVRs (one SVR per feature). The results were then refined with image processing techniques subject to several constraints for enforcing valid reconstructions. Average computation time by itself was of 2.4 min per reconstruction, and user-interaction time was not reported. In the statistical approach of this study, the spine midline (with normalised scale) is the only predictor of the shape of the spine. While this is acceptable, there may be a range of spine shapes for the same spline curve. Additionally, LLE may produce inaccurate predictors for splines that are not sufficiently well sampled, and using a set of independent SVRs does not ensure plausible reconstructions of the spine since each output feature is trained independently, thus, the longitudinal relation between vertebrae is not taken into account.

Recently, Boisvert et al. proposed representing the spine as an articulated model (AM) for conveniently describing spine shape variability [30]. These models capture inter-vertebral variability of the spine geometry by representing vertebrae position and orientation as rigid geometric transformations from one vertebra to the other along the spine. Such models already have proven to be advantageous when only partial data about the shape of the spine is available. In [31] AM were used to infer 3D landmarks of vertebrae for which user input was missing and in [32] an AM enabled inferring 3D reconstructions from a single radiograph (manually labelled).

In this paper we propose a method that balances user-interaction with computational efficiency for providing faster reconstructions than the methods previously published, while ensuring statistically plausible reconstructions. The only user input required by the proposed method is one spline (with about 7 control points) per radiograph defining the vertebral body line. This input is used for guiding the deformation of a statistical model of the shape of the spine built from articulated representations of the spines of 295 scoliotic patients. Using this prior knowledge of spinal shape variability allows to infer the 3D coordinates of 6 points per vertebra from the two input splines. These six points are typically manually identified in highly supervised reconstruction methods [13–15] and allow to determine vertebra location and orientation, as well as clinical indices of the spine, as previously described. For enhancing vertebrae location, the method makes use of the position of the control points of the splines, which were neglected in all the previous approaches. Therefore, the method proposed here provides a more efficient and effective utilisation of the input data, allowing to improve accuracy without requiring additional interaction. This paper also includes a validation study where a thorough comparison is made with state-of-the-art reconstruction methods. We conclude that, to the best of our knowledge, this is the fastest 3D reconstruction method of the spine for biplanar radiography that is able to accurately locate vertebrae while providing the estimation of clinical indices with no significant differences to fully manual approaches.

2. Materials and methods

2.1. X-ray images acquisition

The radiographs used in this study were acquired at Saint-Justine Hospital Centre in Montreal, Canada, with a FCR7501 system (Fuji Medical, Tokyo, Japan), producing 12-bits grayscale digital images with resolution of 2140×880 pixels. Two radiographs were available for each examination, one posterior–anterior (PA) and one lateral (LAT). Patients positioning and radiography calibration was ensured by the system proposed in [7]. In this system, patients wear a vest with 16 radiopaque pellets and are positioned by means of rotatory platform that includes a plate with 6 pellets with known absolute 3D coordinates. The pellets of the plate are used to help determining the orientation of the referential and the scale of the reconstruction, while the pellets of the vest enable to determine the actual geometrical transformation from the first radiograph acquisition to the second, taking into account eventual

patient movement. Three-dimensional reconstructions of the spine were available for all exams utilised in this study. These reconstructions were performed using a previously validated method [15] that determines the 3D position of six anatomical landmarks per vertebra (i.e. centre of superior and inferior endplates, and the superior and inferior extremities of the pedicles) based on manual identification of these points in both PA and LAT radiographs by an expert.

2.2. User interface

User input is limited to placing a few control points for identifying the spine midline in the two radiographs (PA and LAT) using parametric splines (Fig. 1). The splines are calculated from the control points using monotonic piecewise cubic Hermite interpolation [33], which produces splines with continuous first derivative. This class of splines was experimentally found to be more suitable for approximating the spine midline and more predictable for users than cubic splines, which also force the second derivative to be continuous. Nevertheless, the assumption of continuous first derivative may not be met by spines with vertebral fractures, dislocated vertebrae, or with surgical instrumentation that provoke discontinuities of the spinal midline, rendering the proposed method unsuitable for these cases.

Both PA and LAT splines should begin at the centre of the superior endplate of vertebra T1 and should end at the centre of the inferior endplate of L5. These are the only stereo-correspondent points that are required. For helping users to identify these points, the graphical user interface (GUI) can display the epipolar line of a given point in the opposite view.

For enabling full use of the input data, users may place the remaining control points at specific anatomical points, i.e. centre of superior endplates, centre of inferior endplates, or centre of vertebral bodies. Placing control points at particular anatomical features provides input concerning vertebrae location that allows improving reconstruction accuracy. Typically, for faster interaction, users place all control points at a default location, i.e. the centre of superior endplates.

2.3. Statistical model of the spine

For conveniently describing spine shape variability we propose using articulated models (AM) [30]. These models represent vertebrae position and orientation as rigid geometric transformations from one vertebra to the other along the spine. In an articulated representation, only the first vertebra (i.e. L5) has an absolute position and orientation, and the following vertebrae are dependent from their predecessors:

$$T_i^{abs} = T_1 \circ T_2 \circ \cdots \circ T_i, \quad \text{for} \quad i = 1, \ldots, N, \tag{1}$$

where T_i^{abs} is the absolute geometric transformation for vertebra i, T_i is the geometric transformation for vertebra i relative to vertebra $i-1$ (with the exception of the first vertebra), $\circ$ is the composition operator, and N is the number of vertebrae represented by the model.

In order to include data concerning vertebrae morphology, a set of landmarks is expressed in the local coordinate system of each vertebra. The absolute coordinates for each landmark may be calculated as:

$$p_{i,j}^{abs} = T_i^{abs} \star p_{i,j}, \quad \text{for} \quad i = 1, \ldots, N, j = 1, \ldots, M, \tag{2}$$

where $p_{i,j}^{abs}$ are the absolute coordinates for landmark j of vertebrae i, $p_{i,j}$ are the relative coordinates, $\star$ is the operator that applies a transformation to a point, and M is the number of landmarks per vertebra. Thus, an articulated representation of the spine that models both global and local shape may be expressed as a vector that includes inter-vertebral rigid transformations and relative landmarks for each vertebra:

$$s = [T_1, \ldots, T_N, p_{1,1}, \ldots, p_{N,M}]. \tag{3}$$

The method proposed here uses an articulated model of the spine comprised of $N = 17$ vertebrae (from L5 to T1) and $M = 6$ landmarks per vertebra. The first two landmarks are the centre of the superior and inferior endplates ($j = 1, \ldots, 2$) and the remaining four are the superior and inferior extremities of both pedicles ($j = 3, \ldots, 6$). The origin of each vertebra coordinate system is located at the centre of the pedicles' landmarks.

For building a statistical model of the spine, a set of 295 3D reconstructions was first represented in an articulated fashion (see Eq. (3)). Then, centrality and dispersion measures were computed, namely the mean articulated model (μ) and the covariance matrix (Σ). Because of the presence of inter-vertebral rigid transformations, articulated models do not naturally belong to an Euclidian space. Thus, Riemannian statistics [34] were used to compute μ and Σ. The mean articulated model of n articulated models $s_{1,\ldots,n}$ is given by the Fréchet mean, which is computed using the following iterative scheme, until convergence:

$$\mu_{t+1} = \mathrm{Exp}_{\mu_t}\left(\frac{1}{n}\sum_i \mathrm{Log}_{\mu_t}(s_i)\right). \tag{4}$$

The symbols Exp and Log refer to the Riemannian exponential and log maps, which are defined as follows for the articulated models used in the proposed method (see [30] for more details):

$$\mathrm{Log}_{s'}(s) = \left[\Delta t_1, \Delta\theta_1 \Delta a_1, \ldots, \Delta t_N, \Delta\theta_N \Delta a_N, p_{1,1} - p'_{1,1}, \ldots, p_{N,M} - p'_{N,M}\right], \text{ and}$$
$$\mathrm{Exp}_{s'}(s) = \left[T'_1 \circ T(t_1, \theta_1 a_1), \ldots, T'_N \circ T(t_N, \theta_N a_N), p_{1,1} + p'_{1,1}, \ldots, p_{N,M} + p'_{N,M}\right]$$

where $\Delta\theta_i$, Δa_i, and Δt_i respectively designate the angle of rotation, its axis and the translation associated with $T_i'^{-1} \circ T_i$. The function $T()$ returns the rigid transformation formed by a translation combined with a rotation expressed as the product of an axis of rotation and an angle. The covariance matrix (Σ) is then computed in the tangent plane around the mean, such as:

$$\Sigma = \frac{1}{n}\sum_{i=1}^{n} \mathrm{Log}_\mu(s_i)^T \mathrm{Log}_\mu(s_i). \tag{5}$$

2.4. Spline guided deformation of the statistical AM

Three-dimensional reconstructions of the spine based on the user-defined splines are achieved using an optimisation process that iteratively deforms an AM towards minimising the distance between the projected landmarks of the reconstructed model and the splines. Additionally, principal components analysis (PCA) [35] is used for reducing the number of dimensions of the AM, while capturing the main deformation modes.

Using PCA in a linearised space, an articulated representation of a spine s may be generated by linearly combining the eigen-vectors of the covariance matrix and then by composing the result with the mean articulated model:

$$s = \mathrm{Exp}_\mu\left(\sum_i \gamma_i v_i\right) \tag{6}$$

where γ_i is the weight associated with the i th eigenvector of the covariance matrix and v_i is i th eigenvector of the covariance matrix. Finally, the 3D reconstruction of any configuration s may be obtained by first calculating the absolute transformation of each

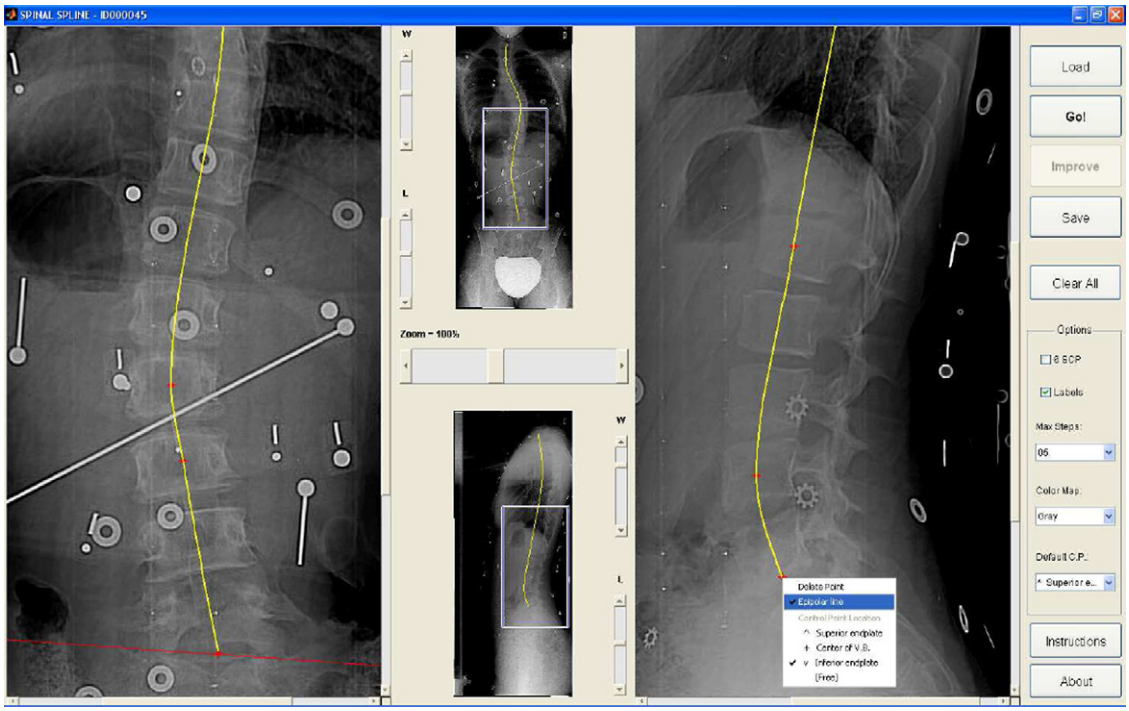

Fig. 1. Graphical user interface (GUI) designed for identifying the splines: this figure illustrates how the GUI may provide epipolar lines; in this case, an epipolar line is drawn on the PA that corresponds to the control point identified on L5 vertebra on the lateral radiograph.

vertebrae (Eq. (1)) and then the absolute 3D position of every landmark (Eq. (2)). Fig. 2 illustrates the influence on the shape of the spine of the first three principal deformation modes of the statistical shape model.

The goal of the optimisation process is to find the values of γ_i that generate the spine configuration s that best fits the user-defined splines of both radiographs. The fitting error was defined as the distance between (a) the absolute position of the endplates of the deformed model and (b) the user-defined splines. For calculating such distance, the endplates of the deformed model are first projected to both radiographs (PA and LAT). Then, for each radiograph, the coordinates of the projected endplates (p^{2D}) have to be mapped to the user-defined spline in order to calculate the distance between endplates and the spline (Fig. 3). The mapped locations $u = \{x_u, y_u\}$ are calculated in the following way:

- y_u are obtained using linear interpolation: the values of the y coordinate of the projected endplates are scaled to fit the height of the user-defined spline;
- x_u are the values of the x coordinate on the user-defined spline at y_u, which are found using piecewise cubic Hermit interpolation [33], assuming that the y coordinate along the spine midline

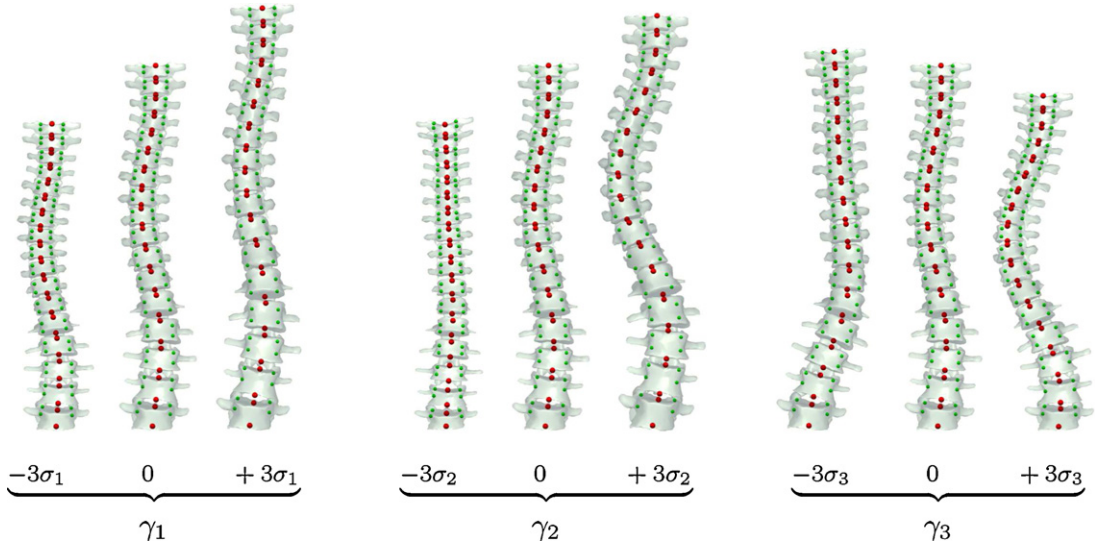

Fig. 2. Effect of varying the weight (γ_i) of each of the first three principal deformation modes of the statistical shape model in turn for −3, 0 (mean model), and 3 times the standard deviation (σ_i) of the deformation mode. The statistical shape model describes the variability of 6 landmarks per vertebrae (endplates – red strong points medially located; pedicles – green small points laterally located) by modeling their relative location, orientation and shape on an articulated fashion. For illustration purposes, 3D models of complete vertebrae were rendered. (For interpretation of the references to colour in this figure legend, the reader is referred to the web version of the article.)

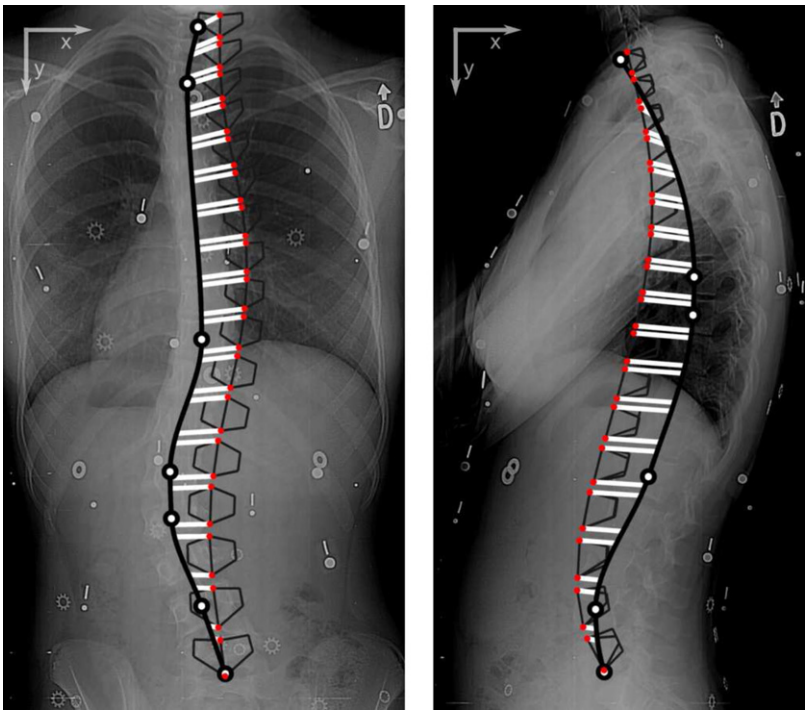

Fig. 3. Fitting error of the deformable AM, calculated as the distance between the endplates of the AM (red dots) and their estimated positions on the user-defined splines. The AM is first projected to the PA and LAT radiographs where the operator identified the splines and then the error (white thick line-segments) is calculated for each endplate on each radiograph. (AM represented by 6 points per vertebra connected using black thin line-segments, and user-defined splines represented by thick black curves with control points as white circles.) (For interpretation of the references to colour in this figure legend, the reader is referred to the web version of the article.)

is monotonically increasing (an alternative capable of handling non-monotonicity at the cost of decreasing computational efficiency was proposed in [36]).

The cost function may now be defined as:

$$C = \sum_{i=1}^{N} \sum_{j=1}^{2} \sum_{k=\{\mathrm{PA,LAT}\}} \left\| p_{i,j,k}^{2D} - u_{i,j,k} \right\|^2, \tag{7}$$

where $p_{i,j,k}^{2D}$ is the projection of the 3D endplates ($p_{i,j}^{abs}$) to radiograph k, and $u_{i,j,k}$ are their estimated locations on the user-defined spline of the same radiograph. Minimising function C is a nonlinear least-squares problem, which is solved with a trust-region algorithm [37]. Trust-region optimisers have shown to be more computational efficient than the traditionally used Levenberg–Marquardt algorithm on least-squares minimisation problems, such as bundle adjustment [38]. Additionally, the adopted trust-region optimiser allows to define bounds for constraining the range of values of the solution [37], which is explored by the method proposed here for ensuring plausible solutions as described in the following section. The trust-region optimiser requires an initial solution that, for this particular problem, is $\gamma_i = 0$ for all principal components, i.e. the initial solution corresponds to the mean model of the spine. Then, the optimiser defines a trust-region around the current solution, and this region is approximated by a quadratic surface, for which a minimum can be directly computed, resulting on a new candidate solution. The algorithm then verifies if there is an actual improvement of the cost by evaluating the cost function with the candidate solution. If there is, the iteration is successful and, thus, the new solution is adopted and the size of the trust-region is increased for the next iteration; otherwise, the iteration is unsuccessful and, consequently, the size of the trust-region is decreased and the solution is not updated. These steps are repeated until convergence.

2.5. Generating plausible spine configurations

The weights γ_i are limited to an hyperellipsoid in the parameter space such that $|\gamma_i| \leq 3\sqrt{\lambda_i}$, being λ_i the eigenvalues of the covariance matrix (Σ). In other words, we limit departures from the mean to three standard deviations to avoid outliers. Moreover, the cost function was modified to include a term that promotes models that are more likely with respect to the prior model. This is done using the Mahalanobis distance [39] on the feature space of the articulated model, which is defined as:

$$D = \sqrt{\mathrm{Log}_{\mu}(s)^T \, \Sigma^{-1} \mathrm{Log}_{\mu}(s)}. \tag{8}$$

Then, the cost function becomes:

$$C = \sum_{i=1}^{N} \sum_{j=1}^{2} \sum_{k=\{\mathrm{PA,LAT}\}} \left\| p_{i,j,k}^{2D} - u_{i,j,k} \right\|^2 + (\alpha D)^2, \tag{9}$$

where α is used for balancing the weight of the prior spine shape knowledge with respect to the spline fitting error. In our experiments, $\alpha = 2.5$ was empirically found to provide a good balance between these two components of the cost function. The value of parameter α essentially depends on the pixel size of the radiographs since the spline error is computed in pixels. Therefore, for other systems this value would have to be adjusted.

2.6. Refinement of vertebrae location

The fitting process just described captures the shape of the spine by placing vertebrae on their probable location along the spine midline, which may not be the correct one since there might be a range of valid arrangements. For improving spine reconstructions without requesting additional information to the user, the location of the control points of the splines are used. However, despite control points being placed at specific anatomical positions (like described

in Section 2.2), it is not known on which vertebrae they lie. For tackling this issue, the two nearest vertebrae of the AM are selected as candidates for each control point after a first minimisation of Eq. (9). Then, the nearest candidate is elected if the level of ambiguity is low enough. This may be formalised in the following way:

$$\frac{d_{m,1}}{d_{m,2}} \leq \omega, \tag{10}$$

where $d_{m,1}$ is the distance of control point m to the nearest candidate of the AM, $d_{m,2}$ is the distance to the second nearest candidate, and ω is a threshold that defines the maximum level of ambiguity allowed. Since $d_{m,1} \leq d_{m,2}$, ambiguity has maximum value of 1 when the candidates are equidistant to the control point, and minimum value of 0 when the nearest candidate is in the exact location of the control point. The list of candidates for a given control point depends on the anatomical position where it was placed, e.g. if a control point was placed on the superior endplate, only the superior endplates of the AM would be candidates for that point.

After determining the set of elected candidates, the optimisation process is repeated, but now including a third component that is added to Eq. (9). This term attracts the elected vertebrae of the articulated model towards their corresponding control points (Fig. 4). Let E be the set of elected candidates, the cost function may be redefined as:

$$C = \sum_{i=1}^{N}\sum_{j=1}^{2}\sum_{k=\{\mathrm{PA,LAT}\}} \left\| p_{i,j,k}^{2D} - u_{i,j,k} \right\|^2 + (\alpha D)^2 + \sum_{m \in E} \left\| d_{m,1} \right\|^2. \tag{11}$$

When the second optimisation finishes, the vertebrae location of the articulated model should be closer to their real position, and some of the ambiguities may be solved. Therefore, several optimisation processes are executed iteratively while the number of elected candidates increases.

Concerning the value of ω, using a low threshold of ambiguity may result in a considerable waste of control points due to an over-restrictive strategy. On the other hand, a high threshold of ambiguity may produce worst results, especially when there are control points placed on erroneous locations. For overcoming this issue, a dynamic thresholding technique is used that begins with a restrictive threshold where only candidates that are at half the distance to the target or less than the second nearest candidate are elected ($\omega = 0.50$). Then, when no candidates are elected, ambiguity is relaxed (by increments of 0.10) up to a maximum threshold ($\omega = 0.70$). If any control points remain ambiguous at this stage, they are considered to be unreliable.

2.7. Method evaluation

Accuracy of spine reconstruction, vertebrae location and rotation, and selected clinical indices were measured for a total of 30 patients: 10 moderate idiopathic scoliosis with Cobb angle in the interval [22°, 43°] and mean value of 33°, and 20 severe idiopathic scoliosis with Cobb angle in the interval [44°, 70°] and mean value of 55°. Acquisition and calibration of the radiographs were done as described in Section 2.1. Reconstructions were performed with the method proposed here by an experienced operator. Accuracy was evaluated by comparison with reconstructions from a previously validated method [14,15] (reference method). The reference method computes the 3D coordinates of 6 anatomical points per vertebrae by triangulating their 2D coordinates on the PA and LAT radiographs, which are manually identified by an experimented operator. These 6 3D points are the same that the method proposed here computes, which allows to make direct comparisons between the two methods. The *in vitro* accuracy of the reference method computing the 3D position of these points is of 1.3 mm [14].

The deformable articulated model was built using 295 3D spine reconstructions (Cobb angle in the interval [4°, 86°]) that did not include any 3D reconstruction of the patients of the testing set. For enhancing computational performance, a different number of principal components were used depending on the stage of the reconstruction method. For the final stage, when there are no ambiguous control points, the principal components that explain 99% of the spine shape variation were used, and in the previous stages only 95% of the components were used.

2.7.1. User interaction versus reconstruction accuracy

The influence of the amount of user input was studied by generating splines with variable number of control points from 5 to 17 per radiograph. Splines were automatically generated using the reference data, in particular, the manually identified endplates. The mean RMS 3D reconstruction error was calculated for the endplates' landmarks as well as for the pedicles' landmarks by comparison with the reference data.

2.7.2. Spine reconstruction accuracy

RMS 3D reconstruction errors were first calculated for each exam and for both endplates and pedicles. Accuracy was measured using the mean, standard deviation and maximum RMS errors for each test set. Results for patients with moderate scoliosis were compared with the values presented in [28] where the same statistics were calculated for a similar sample of patients.

2.7.3. Vertebrae location and orientation accuracy

Accuracy of vertebrae location and orientation was measured as the root mean square of the standard deviation (RMS_{SD}) of the error between reconstructions with the proposed method (observation 1) and the reference data (observation 2), as proposed in [25]:

$$RMS_{SD} = \sqrt{\frac{\sum_{m}\left(\sum_{n}(\bar{\alpha} - \alpha_n)/n\right)^2}{m}}, \tag{12}$$

where $\bar{\alpha}$ is the mean of the $n = 2$ observations, and m is the number of computed locations or orientations about either of the axes. A vertebral reference frame was associated to each vertebra based on the definition of Stokes and the Scoliosis Research Society [1] and was used to assess location and orientation. Results for the moderate scoliosis testing set were compared with [25].

2.7.4. Clinical indices accuracy

Accuracy of the proposed method measuring clinical indices was evaluated as the mean and standard deviation of the differences to the reference method for the following indices: Cobb angle on the PA, Cobb angle on the plane of maximum deformity, orientation of the plane of maximum deformity, kyphosis and lordosis. The computation of these indices, as described in [16], involves computing the 3D curve that passes by the pedicles midpoint of each vertebrae, which is then smoothed using a least-squares fit of a parametric Fourier series. Additionally, a Wilcoxon signed-rank test was performed for identifying if there were significant differences ($p \leq 0.05$) between results of the two methods.

2.7.5. Reconstruction time

Finally, reconstruction time was evaluated by measuring the user interaction time needed for identifying the splines as well as the computation time for delivering the 3D reconstruction. Average times were computed for the two testing sets and comparisons were made with other spline-based methods [25,26,28].

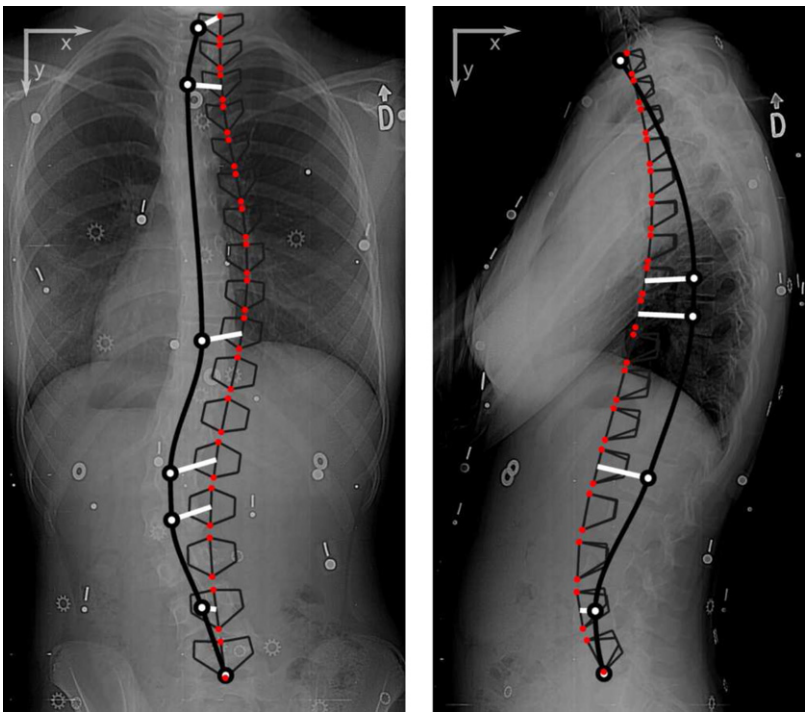

Fig. 4. Using the location of the control points of the splines to improve fitting: since users place each control point over a vertebra, the location of the control point on the radiograph is used to attract the nearest vertebra of the AM. In this illustration all control points were placed at the centre of the vertebral bodies (with the exception of T1 and L5). (AM represented by 6 points per vertebra connected using black thin line-segments, user-defined splines represented by thick black curves with control points as white circles, and distance between control points and their nearest vertebra on the AM represented as white thick line-segments.)

3. Results

3.1. User interaction versus reconstruction accuracy

Results show that the reconstruction accuracy of the endplates increases with the number of control points of the splines, on both moderate and severe scoliosis (Fig. 5). This is particularly observable until a given limit where saturation occurs (e.g. 11 control points on moderate scoliosis). Reconstructions with 5 control points did not conveniently describe the spine midline of 3 of the 20 patients with severe scoliosis. This resulted on 3 bad reconstructions with ambiguities mapping control points to the articulated model, which produced higher reconstruction errors. In all other tests, all ambiguities were completely and correctly solved. Regarding the pedicles, no considerable improvement is observed by increasing the number of control points beyond the minimum necessary to describe the spine midline ($\geq$7 for severe scoliosis). Comparison between the two test sets, for a number of control points $\geq$7, revealed that reconstruction errors on the endplates were on average 0.2 mm higher on the severe test set, while on the pedicles this difference was of 0.5 mm.

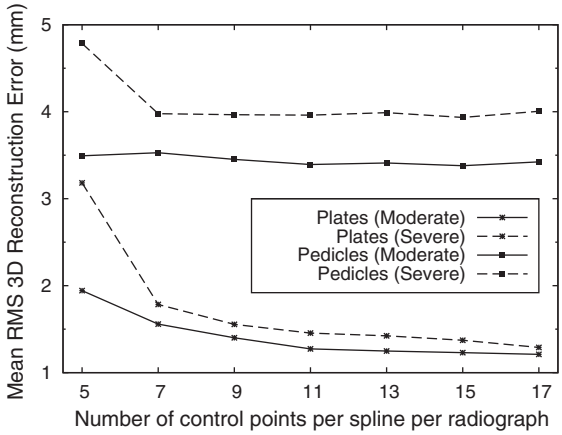

Fig. 5. Mean RMS 3D reconstruction error versus number of control points per spline per radiograph.

3.2. Spine reconstruction accuracy

Results show average RMS reconstruction errors of 2.0 mm and 2.1 mm on the endplates' landmarks for moderate and severe scoliosis respectively (Table 1). Reconstruction errors of the pedicles were higher on severe scoliosis (4.0 mm) when compared with moderate scoliosis (3.5 mm). Pedicles' reconstruction errors were higher than endplates' reconstruction errors on all patients. The maximum reconstruction error was observed on the patient with the highest Cobb angle.

The operator identified an average of 7 control points on both PA and lateral radiographs when reconstruction patients with moderate scoliosis, and an average of 9 control points on the PA and 7 on the lateral for severe scoliosis. The majority of control points were placed on the centre of the superior endplate and only on a few vertebrae the operator choose to place control points on the bottom endplate. The proposed method was always able to solve the ambiguities when mapping control points to vertebrae of the articulate model, and therefore all control points were always used for refining vertebrae location.

3.3. Vertebrae position and orientation accuracy

Results for this experiment are presented in Table 2 and show that the proposed method presents no considerable differences between moderate and severe scoliosis when locating vertebrae position. Regarding orientation, the same was observed for rotations about all axes with the exception of axial rotation (Z axis)

Table 1
RMS reconstruction errors for the six 3D points per vertebrae, i.e. Plates (centre of superior and inferior endplates) and pedicles (superior and inferior extremities of the left and right pedicles), for the severe and moderate scoliosis test sets, and comparison with the method proposed by Kadoury et al. [28].

Method	*N*	Cobb angle [min–max]	Mean ± SD [max] 3D error (mm)	
			Plates	Pedicles
Proposed	20	[44–70°] (severe)	2.1 ± 0.3 [2.9]	4.0 ± 0.9 [6.1]
Proposed	10	[22–43°] (moderate)	2.0 ± 0.3 [2.3]	3.5 ± 0.4 [4.3]
Kadoury et al. [28]	20	[15–40°] (moderate)	2.2 ± 0.9 [4.7]	2.0 ± 1.5 [5.5]

Table 2
RMS_{SD} location and orientation errors for the severe and moderate scoliosis test sets, and comparison with the method proposed by Dumas et al. [25] (orientation is expressed as a rotation about the given axis).

Method	*N*	Mean Cobb angle	Location (mm)			Orientation (°)		
			X	*Y*	*Z*	*X*	*Y*	*Z*
Proposed	20	55° (severe)	0.6	0.5	0.5	1.2	1.5	4.4
Proposed	10	33° (moderate)	0.5	0.5	0.4	1.2	1.3	3.3
Dumas et al. [25]	11	30° (moderate)	0.9	1.1	2.3	1.3	2.0	3.2

where errors on severe scoliosis (4.4°) were higher than errors on moderate scoliosis (3.3°).

3.4. Clinical indices accuracy

Results for this experiment are presented in Table 3 and show that no significant differences were found for all evaluated clinical indices on patients with moderate scoliosis ($p \leq 0.05$). On severe scoliosis, Cobb angle at the maximum plane of deformation and Kyphosis shown statistically significant differences, both with $p = 0.03$.

3.5. Reconstruction time

Average reconstruction times, for both user interaction and reconstruction computation, are presented in Table 4. Computation times were measured on a Desktop PC with an AMD Phenom II X2 550 3.10 GHz processor and 2 GBytes of memory for an implementation on Matlab of the proposed method.

4. Discussion

The method proposed by Kadoury et al. [28] is probably the spline-based method with higher accuracy of 3D reconstruction for patients with moderate scoliosis. However, it requires considerable computation time (2.4 min) in addition to the interaction time needed for identifying the splines. This method finds an initial reconstruction using a statistical approach that is refined using image processing subject to several restrictions. Comparison with the proposed method (Table 1) shows comparable mean reconstruction errors of the endplates for a similar sample (moderate scoliosis), while requiring much less computation time (~3 s). Additionally, the proposed method achieves lower standard deviation (0.3 mm vs 0.9 mm) and lower maximum error (2.3 mm vs 4.7 mm) for the endplates, which demonstrates more robustness locating these landmarks. Moreover, when testing the method on patients with severe scoliosis, the endplates' results remain more robust than the results presented in [28] for moderate scoliosis. Concerning pedicles reconstruction, the method presented here achieves higher mean reconstruction errors (3.5 mm vs 2.0 mm), since they are completely inferred by the statistical model with no direct clues from the operator nor from the content of the radiographic images. Nevertheless, the proposed method presents much lower standard deviation (0.4 mm vs 1.5 mm) and lower maximum error (4.3 mm vs 5.5 mm), which again shows more stable results despite the average error being higher.

It is also important to mention that the method proposed by Kadoury et al. uses a considerably larger database for creating the statistical model (732 exams vs 295 exams), which may have direct impact on results. This was needed since the statistical approach proposed by the authors is based on local linear embedding (LLE) and this technique is sensible to insufficient sampling [40]. In fact, despite LLE and several other dimensionality reduction techniques showing good results on artificial datasets, experiments with real-world data show that PCA often outperforms them [40]. Therefore, the method proposed here should be able to better modelling the population when fewer cases are available for building the statistical model, which may happen on other kinds of deformities, or in institutions without access to such amount of data.

Simulation results (Fig. 5) enabled to conclude that having more control points enables improving the accuracy of the reconstruction of the endplates' centres. Therefore, reconstruction accuracy could be superior if the operator had chosen to identify more control points. This creates a tradeoff between reconstruction accuracy and interaction time that may be adjusted according to users' needs and the objective of the examination. However, these results also show that this additional interaction may have no effect on the accuracy of the reconstruction of pedicles.

Comparison with the results presented by Dumas et al. [25] shows that vertebrae location accuracy was considerably improved by our method (Table 2) while requiring less interaction (1.5 min vs 5 min). Moreover, results with severe scoliosis were comparable with moderate scoliosis, which shows the method ability for locating vertebrae even on more severe cases. In terms of vertebrae orientation, results were comparable with the ones presented in Dumas et al. with the exception of vertebrae rotation on *Y* axis that was more accurately estimated by our method. Axial rotation is considerably less accurately estimated than rotations about *X* and *Y* axes, and is sensible to an increase on the severity of scoliosis. This was expected since, unlike the rotation about *X* and *Y* axes that are calculated with the reconstructed endplates only, axial rotation is calculated using the reconstructed pedicles, which have inferior accuracy. Nevertheless, the estimation of axial rotation with the reference method has higher inter-user variability than the remaining rotations even on *in vitro* experiments [41]. These errors tend to increase on *in vivo* scenarios due to difficulties identifying pedicles, making the inter/intra-user variablity on the apical vertebrae raising up to 8° [15]. Consequently, it is difficult to properly quantify the accuracy of pedicles' reconstruction as well as axial rotation.

A proper comparison with the method proposed in Humbert et al. [26] was not possible since the authors did not perform an accuracy study on neither vertebrae location, orientation, nor

Table 3
Average differences between the proposed and the reference method [14,15] for clinical indices and results of the Wilcoxon signed-rank test: S – significant difference, NS – non-significant difference at $p \leq 0.05$ ($Cobb_{PA}$ – Cobb angle on the PA, $Plane_{Max}$ – plane of maximum deformity, $Cobb_{Max}$ – Cobb angle on the $Plane_{Max}$).

Index	Moderate		Severe	
	Mean ± SD difference	p	Mean ± SD difference	p
$Cobb_{PA}$(°)	0.4 ± 3.1	0.85 (NS)	1.0 ± 2.4	0.09 (NS)
$Cobb_{Max}$(°)	0.7 ± 4.9	0.70 (NS)	1.6 ± 2.8	0.03 (S)
$Plane_{Max}$(°)	2.7 ± 17.7	0.64 (NS)	1.5 ± 16.2	0.57 (NS)
Kyphosis(°)	−1.2 ± 5.7	0.92 (NS)	0.9 ± 1.6	0.03 (S)
Lordosis(°)	2.2 ± 4.6	0.16 (NS)	0.0 ± 5.8	0.91 (NS)

Table 4
Average reconstruction time (min:s) comparison with other spline-based methods for patients with moderate scoliosis (statistics for severe scoliosis are included inside brackets when available).

	Proposed	Kadoury et al. [28]	Humbert et al. [26]	Dumas et al. [25]
User interaction	1:30 [1:50]	n.a.	2:30 [3:00]	5:00
Computation	0:03 [0:03]	2:24	0:04 [0:04]	n.a.

clinical indices. Nevertheless, the method presented here has considerably less user interaction (∼1 min less). Moreover, the times presented in [26] benefit from radiographs captured with superior image quality and with no image distortion along the Z axis due the use of an EOS system [42] instead of standard radiographic equipment with cone-beam X-rays. These features of the EOS facilitate the identification of the splines as well as of anatomical features, which may contribute for faster times and higher accuracy.

Results of the accuracy study of clinical indices (Table 3) show that no significant differences were found for patients with moderate scoliosis ($p \leq 0.05$). Despite there is a large variation on the orientation of the plane of maximum deformation, inter-observer precision of the reference method reaches a variability of 20.4° [15]. On the test set of severe scoliotic patients, two indices presented significant differences: the Cobb angle at the maximum plane of deformity and the angle of kyphosis. However, both these indices present acceptable mean differences for clinical practice. Additionally, the inter-observer variability of kyphosis for the reference method is of 2.8°. Therefore, it is possible to conclude that the method presented here is suitable for clinical evaluation of both moderate and severe scoliosis (Cobb angle up to 70°).

5. Conclusion

This study proposed and assessed a novel 3D reconstruction method of the scoliotic spine based on deformable articulated models. The method is based on two fundamental concepts: (i) the ability of articulated models for inferring missing information and (ii) the exploration of the position of the splines' control points for improving reconstruction accuracy without considerably increasing interaction time. To the best of our knowledge, these two features enabled us to achieve the fastest reconstructions as well as the highest accuracy locating the vertebral bodies and the centres of their endplates, which enabled a proper estimation of clinical indices. Therefore, the proposed method makes possible having rapid and accurate feedback at the moment of examination, something of crucial importance for today's requirements of clinical institutions. In addition, computation time may be considerably decreased by calculating the derivatives of the cost function analytically, instead of using finite differences. This would enable users to have reconstructions as they identify control points, which would allow to interactively refining reconstructions.

Future work includes improving pedicles 3D reconstruction using image processing techniques. This challenging problem is now easier to address since, with the proposed method, vertebral bodies are well localised, and initial estimates of the pedicles location are available, which helps limiting the region of interest in the radiographs.

Acknowledgements

The authors would like to express their gratitude to Farida Cheriet, Lama Séoud and Hassina Belkhous from École Polytechnique de Montréal, Canada, for their valuable contribution on the validation process.

The first author thanks Fundação para a Ciência e a Tecnologia (FCT), Portugal, for his PhD scholarship (SFRH/BD/31449/2006), and Fundação Calouste Gulbenkian, Portugal, for granting his visit to École Polytechnique de Montréal.

This work was partially done in the scope of the projects "Methodologies to Analyze Organs from Complex Medical Images - Applications to Female Pelvic Cavity", "Aberrant Crypt Foci and Human Colorectal Polyps: mathematical modelling and endoscopic image processing" and "Cardiovascular Imaging Modeling and Simulation - SIMCARD", with references PTDC/EEA-CRO/103320/2008, UTAustin/MAT/0009/2008 and UTAustin/CA/0047/2008, respectively, financially supported by FCT.

Conflict of interest

None.

References

[1] Stokes IA. Three-dimensional terminology of spinal deformity. a report presented to the scoliosis research society by the scoliosis research society working group on 3-D terminology of spinal deformity. Spine 1994;19(2):236–48.
[2] Yazici M, Acaroglu E, Alanay A, Deviren V, Cila A, Surat A. Measurement of vertebral rotation in standing versus supine position in adolescent idiopathic scoliosis. J Pediat Orthopaed 2001;21(2):252–6.
[3] Levy A, Goldberg M, Mayo N, Hanley J, Poitras B. Reducing the lifetime risk of cancer from spinal radiographs among people with adolescent idiopathic scoliosis. Spine 1996;21(13):1540–7.
[4] Dansereau J, Stokes I. Measurements of the three-dimensional shape of the rib cage. J Biomech 1988;21(11):893–901.
[5] Dumas R, Mitton D, Laporte S, Dubousset J, Steib JP, Lavaste F, et al. Explicit calibration method and specific device designed for stereoradiography. J Biomech 2003;36(6):827–34.
[6] Kadoury S, Cheriet F, Laporte C, Labelle H. A versatile 3D reconstruction system of the spine and pelvis for clinical assessment of spinal deformities. Med Biol Eng Comput 2007;45(6):591–602.
[7] Cheriet F, Laporte C, Kadoury S, Labelle H, Dansereau J. A novel system for the 3-D reconstruction of the human spine and rib cage from biplanar X-ray images. IEEE Trans Biomed Eng 2007;54(7):1356–8.
[8] Moura DC, Barbosa JG, Reis AM, Tavares JMRS. A flexible approach for the calibration of biplanar radiography of the spine on conventional radiological systems. Comput Model Eng Sci 2010;60(2):115–38.
[9] Labelle H, Dansereau J, Bellefleur C, Poitras B. Three-dimensional effect of the boston brace on the thoracic spine and rib cage. Spine 1996;21(1):59–64.

[10] Labelle H, et al. Comparison between preoperative and postoperative three-dimensional reconstructions of idiopathic scoliosis with the cotrel-dubousset procedure. Spine 1995;20(23):2487–92.
[11] Villemure I, Aubin C, Grimard G, Dansereau J, Labelle H. Progression of vertebral and spinal three-dimensional deformities in adolescent idiopathic scoliosis: a longitudinal study. Spine 2001;26(20):2244–50.
[12] Labelle H, Bellefleur C, Joncas J, Aubin C, Cheriet F. Preliminary evaluation of a computer-assisted tool for the design and adjustment of braces in idiopathic scoliosis: a prospective and randomized study. Spine 2007;32(8):835–43.
[13] Aubin CE, Descrimes JL, Dansereau J, Skalli W, Lavaste F, Labelle H. Geometrical modelling of the spine and thorax for biomechanical analysis of scoliotic deformities using finite element method. Ann Chir 1995;49(8):749–61.
[14] Aubin C, Dansereau J, Parent F, Labelle H, de Guise JA. Morphometric evaluations of personalised 3D reconstructions and geometric models of the human spine. Med Biol Eng Comput 1997;35(6):611–8.
[15] Delorme S, Petit Y, de Guise J, Labelle H, Aubin CE, Dansereau J. Assessment of the 3-D reconstruction and high-resolution geometrical modeling of the human skeletal trunk from 2-D radiographic images. IEEE Trans Biomed Eng 2003;50(8):989–98.
[16] Labelle H, Dansereau J, Bellefleur C, Jéquier J. Variability of geometric measurements from three-dimensional reconstructions of scoliotic spines and rib cages. Eur Spine J 1995;4(2):88–94.
[17] Trochu F. A contouring program based on dual kriging interpolation. Eng Comput 1993;9(3):160–77.
[18] Mitton D, Landry C, Vron S, Skalli W, Lavaste F, De Guise J. 3D reconstruction method from biplanar radiography using non-stereocorresponding points and elastic deformable meshes. Med Biol Eng Comput 2000;38(2):133–9.
[19] Mitulescu A, Semaan I, De Guise J, Leborgne P, Adamsbaum C, Skalli W. Validation of the non-stereo corresponding points stereoradiographic 3D reconstruction technique. Med Biol Eng Comput 2001;39(2):152–8.
[20] Mitulescu A, Skalli W, Mitton D, De Guise J. Three-dimensional surface rendering reconstruction of scoliotic vertebrae using a non stereo-corresponding points technique. Eur Spine J 2002;11(4):344–52.
[21] Bras AL, Laporte S, Mitton D, de Guise JA, Skalli W. Three-dimensional (3D) detailed reconstruction of human vertebrae from low-dose digital stereoradiography. Eur J Orthopaed Surg Traumatol 2003;13(2):57–62.
[22] Pomero V, Mitton D, Laporte S, de Guise JA, Skalli W. Fast accurate stereoradiographic 3D-reconstruction of the spine using a combined geometric and statistic model. Clin Biomech 2004;19(3):240–7.
[23] Benameur S, Mignotte M, Parent S, Labelle H, Skalli W, de Guise J. 3D/2D registration and segmentation of scoliotic vertebrae using statistical models. Comput Med Imaging Graphics 2003;27(5):321–37.
[24] Benameur S, Mignotte M, Labelle H, Guise JAD. A hierarchical statistical modeling approach for the unsupervised 3-D biplanar reconstruction of the scoliotic spine. IEEE Trans Biomed Eng 2005;52(12):2041–57.
[25] Dumas R, Blanchard B, Carlier R, de Loubresse C, Le Huec J, Marty C, et al. A semi-automated method using interpolation and optimisation for the 3D reconstruction of the spine from bi-planar radiography: a precision and accuracy study. Med Biol Eng Comput 2008;46(1):85–92.
[26] Humbert L, Guise JD, Aubert B, Godbout B, Skalli W. 3D reconstruction of the spine from biplanar X-rays using parametric models based on transversal and longitudinal inferences. Med Eng Phys 2009;31(6):681–7.
[27] Vaiton M, Dansereau J, Grimard G, Beauséjour M, Labelle H, de Guise J. Évaluation d'une méthode clinique d'acquisition rapide de la géométrie 3D de colonnes vertébrales scoliotiques. ITBM-RBM 2004;25(3):150–62.
[28] Kadoury S, Cheriet F, Labelle H. Personalized x-ray 3D reconstruction of the scoliotic spine from hybrid statistical and image-based models. IEEE Trans Med Imaging 2009;28(9):1422–35.
[29] Roweis S, Saul L. Nonlinear dimensionality reduction by locally linear embedding. Science 2000;290(5500):2323–6.
[30] Boisvert J, Cheriet F, Pennec X, Labelle H, Ayache N. Geometric variability of the scoliotic spine using statistics on articulated shape models. IEEE Trans Med Imaging 2008;27(4):557–68.
[31] Boisvert J, Cheriet F, Pennec X, Labelle H, Ayache N. Articulated spine models for 3-D reconstruction from partial radiographic data. IEEE Trans Biomed Eng 2008;55(11):2565–74.
[32] Boisvert J, Cheriet F, Pennec X, Ayache N. 3D reconstruction of the human spine from radiograph(s) using a multi-body statistical model. Prog Biomed Opt Imaging 2009;10(37).
[33] Fritsch F, Carlson R. Monotone piecewise cubic interpolation. SIAM J Numer Anal 1980;17(2):238–46.
[34] Pennec X. Intrinsic statistics on Riemannian manifolds: Basic tools for geometric measurements. J Math Imaging Vision 2006;25(1):127–54.
[35] Jolliffe I. Principal component analysis. 2nd ed. New York: Springer Verlag; 2002.
[36] Moura DC, Boisvert J, Barbosa JG, Tavares JMRS. Fast 3D reconstruction of the spine using user-defined splines and a statistical articulated model. In: Advances in visual computing; vol. 5875 of LNCS. 2009. p. 586–95.
[37] Coleman TF, Li Y. An interior trust region approach for nonlinear minimization subject to bounds. SIAM J Optim 1996;6(2):418–45.
[38] Lourakis M, Argyros A. Is Levenberg–Marquardt the most efficient optimization algorithm for implementing bundle adjustment? IEEE international conference on computer vision, vol. 2. 2005. p. 1526–31.
[39] Maesschalck RD, Jouan-Rimbaud D, Massart DL. The Mahalanobis distance. Chemometrics Intel Lab Systems 2000;50(1):1–18.
[40] van der Maaten L, Postma E, van den Herik J. Dimensionality reduction: a comparative review. J Mach Learn Res 2009;10:1–41.
[41] Dumas R, Le Bras A, Champain N, Savidan M, Mitton D, Kalifa G, et al. Validation of the relative 3D orientation of vertebrae reconstructed by bi-planar radiography. Med Eng Phys 2004;26(5):415–22.
[42] Dubousset J, Charpak G, Dorion I, Skalli W, Lavaste F, Deguise J, et al. A new 2D and 3D imaging approach to musculoskeletal physiology and pathology with low-dose radiation and the standing position: the eos system. Bull l'Acad Natl Méd 2005;189(2):287–97.